Mediterranean nascent sea spray organic aerosol and relationships with seawater biogeochemistry

Evelyn Freney[1], Karine Sellegri[1], Alessia Nicosia[1] , Jonathan T. Trueblood[1], Matteo. Rinaldi[3],

Leah. R. Williams[4], André. S. H. Prévôt[5], Melilotus Thyssen[6], Gérald Grégori[6], Nils

Haëntjens[7], Julie Dinasquet[8, 9*], Ingrid Obernosterer[9], France Van-Wambeke[6], Anja Engel[10],

Birthe Zäncker[10], Karine Desboeufs[11], Eija Asmi[2], Hilka Timmonen[2], Cécile Guieu[12]

[1] Université Clermont Auvergne, CNRS, Laboratoire de Météorologie Physique (LaMP) F-63000 Clermont-Ferrand, France

[2] Atmospheric Composition Research, Finnish Meteorological Institute, Helsinki, FI-00101, Finland

[3] National Research Council (CNR), Institute of Atmospheric Sciences and Climate (ISAC), Bologna, Italy

[4] Aerodyne Research, Inc., Billerica, Massachusetts, USA

[5] Laboratory of Atmospheric Chemistry, Paul Scherrer Institute, 5232 Villigen PSI, Switzerland

[6] Aix-Marseille University, Toulon University, CNRS, IRD, Mediterranean Institute of Oceanography UM110, Marseille 13288, France

[7] School of Marine Sciences, University of Maine, Orono, ME 04469, USA
[8] Marine Biology Research Division, Scripps Institution of Oceanography, 92037 La Jolla, US

[9] CNRS, Sorbonne Université, Laboratoire d'Océanographie Microbienne, UMR7621, F-66650 Banyuls-sur-Mer, France

[10] GEOMAR, Helmholtz Centre for Ocean Research Kiel, 24105 Kiel, Germany
[11] LISA, CNRS UMR7583, Université Paris Est Créteil (UPEC), Université de Paris, Institut Pierre Simon Laplace (IPSL), Créteil, France

[12] Sorbonne Université, CNRS, Laboratoire d'Océanographie de Villefranche, LOV, F-06230 Villefranche-sur-Mer, France

*now at Center for Aerosol Impacts on Chemistry of the Environment, CASPO, Scripps Institution of Oceanography, UCSD, USA

Correspondence to:evelyn.freney@uca.fr

Abstract

The organic mass fraction from sea spray aerosol (SSA) is currently a subject of intense research. The majority of this research is dedicated to measurements in ambient air, although recently a small number of studies have additionally focused on nascent sea spray aerosol. This work presents measurements collected during a five-week cruise in May and June, 2017 in the central and western Mediterranean Sea, an oligotrophic marine region with low phytoplankton biomass. Surface seawater was continuously pumped into a bubble bursting apparatus to generate nascent sea spray aerosol. Size distributions were measured with a differential mobility particle sizer (DMPS). Chemical characterization of the submicron aerosol was performed with a time of flight aerosol chemical speciation monitor (ToF-ACSM) operating with a 15-minute time resolution, and with filter-based chemical analysis on a daily basis. Using a positive matrix factorization analysis, the ToF-ACSM non-refractory organic matter (OM_{NR}) was separated into four different organic aerosols types which were identified as primary

39 OA (POA$_{NR}$), oxidized OA (OOA$_{NR}$), a methanesulfonic acid type OA (MSA-OA$_{NR}$) and a mixed OA (MOA$_{NR}$).
40 In parallel, surface seawater biogeochemical properties were monitored providing information on phytoplankton
41 cell abundance and seawater particulate organic carbon (one-hour time resolution), and seawater surface
42 microlayer (SML) dissolved organic carbon (DOC) (on a daily basis). Statistically robust correlations (for
43 n>500) were found between MOA$_{NR}$ and nano phytoplankton cell abundance, as well as between POA$_{NR}$,
44 OOA$_{NR}$ and particulate organic carbon (POC). Filter-based analysis of the submicron SSA showed that the non-
45 refractory organic mass represented only 13±3% of the total organic mass, which represents 22±6% of the total
46 sea spray mass. Parameterizations of the contributions of different types of organics to the submicron nascent sea
47 spray aerosol, are proposed as a function of the seawater biogeochemical properties for use in models.

48 **1 Introduction**
49 Oceans cover approximately 70% of the Earth's surface and sea spray emissions contribute up to 6 kTons/Yr of
50 particulate matter, making them a major primary source in the atmosphere. The majority of the mass associated
51 with sea spray emissions is in the form of coarse mode sea salt particles. However, it is now well known that the
52 submicron fraction of marine emissions is also important and contains a significant portion of organic
53 compounds (Facchini et al., 2008). This organic fraction tends to be highest during phytoplankton bloom events
54 (O'Dowd et al., 2004). Although the organic fraction of the aerosol population represents little mass, the high
55 number concentration of these aerosol particles makes them a significant contributor to the potential cloud
56 condensation nuclei concentration (Burrow et al. 2018). Organics in sea spray have also been shown to
57 contribute to potential marine ice nuclei (McCluskey et al., 2017). Understanding how the organic fraction of
58 marine aerosol particles transfer to the atmosphere is essential to help identify the contribution of the marine
59 aerosols to the Earth's radiative budget.

60 In general, sea spray aerosol is generated through bubble bursting after wave breaking at the ocean surface, a
61 process that has been described in early publications (Blanchard and Woodcock, 1980). Once bubbles burst, film
62 and jet droplets are ejected into the atmosphere, and dry to leave aerosol particles as residues containing the
63 different constituents of the bulk seawater and surface microlayer. The size distribution of this sea spray extends
64 from the fine particle range, with diameters < 100 nm to the super-micron range (up to 3 μm). The super-micron
65 range is known to be mainly composed of refractory NaCl and different MgCO$_3$ or (Mg)$_2$SO$_4$ species, while the
66 submicron fraction tends to be enriched with organic compounds (O'Dowd et al., 2004).

67 Traditionally, measurements in and around the marine boundary layer were made using offline filter
68 measurements followed by laboratory-based analysis using either ion chromatography or organic carbon and
69 elemental carbon analysis. However, over the last decade, there has been a significant increase in the number of
70 studies deploying online aerosol mass spectrometry methods, including laser ablation mass spectrometry
71 (Dall'Osto et al., 2019) and thermal vaporization followed by electron impact ionization methods (Giordano et
72 al., 2017; Ovadnevaite et al., 2011; Schmale et al., 2013).

73 The aerosol mass spectrometer (AMS, Aerodyne Research, Inc) and aerosol chemical speciation monitor
74 (ACSM) are examples of the latter type and are widely used instruments to monitor the chemical composition of
75 submicron particulate matter in the atmosphere. The design of this instrument is optimized to investigate the
76 non-refractory fraction, defined as material that vaporizes at 600°C of aerosol mass in the atmosphere. In the

77 majority of atmospheric environments, the submicron fraction of the aerosol is dominated by non-refractory

78 organic and inorganic species. In marine environments, the AMS has also been shown to be a useful tool in

79 characterizing submicron sea-salt aerosols (Ovadnevaite et al., 2011) and even more so organic aerosols related

80 to marine emissions.

81 Aerosol mass spectrometry has been used recently to better characterize the chemical properties of ambient

82 marine aerosol particles, from the Atlantic (Ovadnevaite et al., 2011), to Antarctic (Schmale et al., 2013,

83 Giordano et al., 2017) coastal environments. Using a combination of high-resolution aerosol mass spectrometry

84 and positive matrix factorization analysis, different marine organic aerosols have been identified including

85 secondary marine organic aerosols, methanesulfonic acid (MSA), containing organic aerosols, and amino acid

86 (AA) associated organic aerosols thought to be primarily linked to local sea life emissions at the measurement

87 site.

88 Most of these studies measured ambient aerosol already modified through atmospheric chemical and physical

89 processes. Current knowledge on the source and evolution of nascent sea spray organic emissions is still limited.

90 This is attributed to the natural variability of marine organic aerosol and to the lack of high temporal resolution

91 studies at the ocean/atmospheric interface. A very limited number of studies have focused directly on the

92 composition of nascent sea spray aerosol particles emitted from wave action in controlled simulation chambers

93 (Wang et al., 2015) or through dedicated bubble bursting experiments (Bates et al., 2012; Dall'Osto et al., 2019).

94 These studies in controlled environments identified the presence of aliphatic-rich and amino acid-rich organic

95 aerosols related to different phases of phytoplankton blooms (Bates et al. 2012; Wang et al., 2015). Dall'Osto et

96 al., (2019) identified an amino acid contribution in both nascent sea spray aerosol and ambient aerosols.

97 In this work, we characterized nascent sea spray submicron aerosol generated from the underway seawater

98 system of the R/V Pourquoi Pas? over a five-week campaign in the Mediterranean Sea. The Mediterranean Sea

99 is a low nutrient low chlorophyll (LNLC) environment and was characterized by oligotrophic conditions along

100 the whole field campaign (Guieu et al., 2020). Understanding the formation of nascent sea spray aerosols in such

101 an LNLC system can provide valuable information and be extrapolated to other oligotrophic environments.

102 **2-Methodology**

103 **2.1 The PEACETIME oceanographic campaign**

104 The French research vessel, the R/V 'Pourquoi Pas?', was deployed for a five-week-long period from the 10th of

105 May to the 10th of June 2017 on the Mediterranean Sea, as part of the project: PEACETIME (ProcEss studies at

106 the Air-sEa Interface after dust deposition in The Mediterranean sea) project. The ship track (Fig. 1) started and

107 ended in La Seyne sur Mer, France. The ship traveled clockwise covering latitudes in the Mediterranean Sea

108 from 35° to 42°, and longitudes from 0° to 21°.

109 La Seyne s/Mer, France.

110
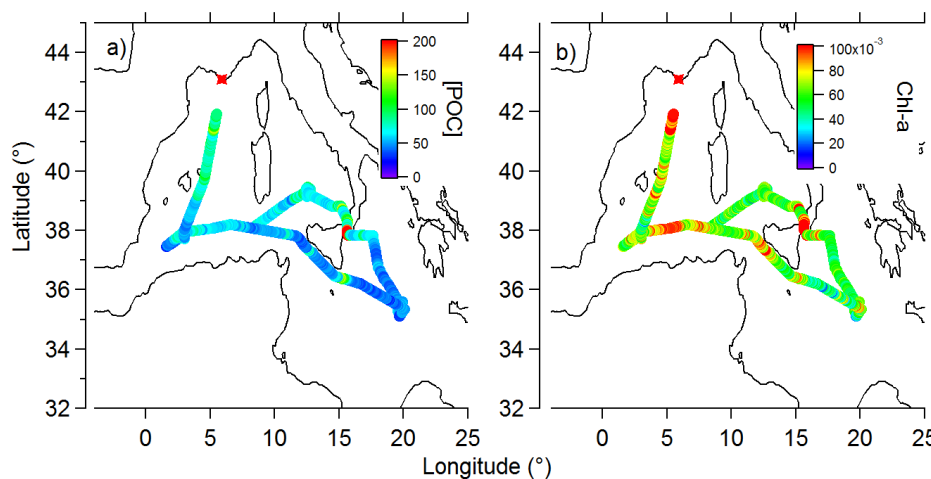
Figure 1: The ship track in the Mediterranean Sea during the PEACETIME expedition. The trajectory is colored by a) POC b) *Chl-a*. . The red star indicates the location of the starting point La Seyne sur Mer.

Results from a suite of hydrology and biogeochemistry measurements performed on board are given in Guieu et al. (2020). In addition to standard seawater temperature (T) and salinity (S) measurements, the concentrations of a wide range of chemical and microbiological parameters were monitored hourly. Several plankton functional groups were identified, including Synechococcus, Prochlorococcus, nanoeurkaryotes, Coccolithophores-like, Cryptophytes-like, and microphytoplankton. The sea surface temperature (T) showed a gradual increase from the start to the end of the campaign from 19°C up to 23°C. Sea surface salinity (S) varied from 36 up to 39 g l^{-1} increasing from east to west. The sampling region was characteristic of open sea (average depth 2750 m ± 770 m along the transect). The sea was calm to moderately rough throughout the sampling period with conditions always remaining below Beaufort 4. Wind speed varied between 10 and 20 m s^{-1}.

Total chlorophyll-a (*Chl-a*) and particulate organic carbon (POC) were also measured. In line with the oligotrophic state of the Mediterranean Sea during this period. POC concentrations were highest at the most northern longitudes and gradually decreased along the ship transect (Fig. 1a), the *Chl-a* concentration remained stable and low (0.07 ±0.03 mg m^{-3}) throughout the sampling period (Fig. 1b).

2.2. Surface Seawater Analysis

2.2.1. Flow cytometry

Phytoplankton cells were counted with one-hour time resolution using an automated Cytosense flow cytometer (Cytobuoy, NL), connected to a continuous clean pumping underway seawater system, as described in Thyssen et al. (2010) and Leroux et al. (2017). Particles were brought within a laminar flow filtered seawater sheath fluid, and detected with forward scatter (FWS) and sideward scatter (SWS) as well a fluorescence in the red (FLR >652 nm) and orange (FLO 552-652 nm) in the size range 1- 800 μm. Two trigger levels were applied for the distinction between highly concentrated picophytoplankton and cyanobacteria groups (trigger level FLR 7.34

135 mV, sampling at a speed of 4 mm³.s⁻¹ and analyzing 0.65 ± 0.18 cm³), and lower concentrated nano- and micro

135 mV, sampling at a speed of 4 mm^3.s^{-1} and analyzing 0.65 ± 0.18 cm^3), and lower concentrated nano- and micro

136 phytoplankton (trigger level FLR 14.87 mV, at a speed of 8 mm^3.s^{-1} and analyzing 3.57 ± 0.97 cm^3). Different

137 sets of 2D projections were plotted in Cytoclus® software to manually gate phytoplankton groups. To follow

138 stability of the flow cytometer, 2 µm red fluorescing polystyrene beads (Polyscience) were regularly analyzed.

139 The use of silica beads (1, 2, 3, 5, 7 *µm in* diameter, Bangs Laboratory) for size retrieving estimates from FWS

140 were used to separate picoplankton from nanoplankton clusters.

141 **2.2.2. Chlorophyll-a and POC**

142 From the underway seawater system, *Chl-a* was derived from the particulate absorption spectrum line-height at

143 676 nm (Bloss et al., 2013) after the relationship was adjusted to PEACETIME *Chl-a* derived from HPLC (*Chl-a*

144 = 194.41 × line_height$^{1.131}$). POC was estimated from particulate attenuation at 660 nm using an empirical

145 relationship specific to PEACETIME (POC = 1405.1 × c$_p$(660) − 52.4) slightly higher than the literature value

146 which is likely due to the small dynamic range (1.27 higher on average for the range observed (Cetinic et al.,

147 2012)). Both particulate attenuation and absorption of surface water were measured continuously with a

148 WetLabs Spectral Absorption and Attenuation Meter using a flow-through system similar to the setup described

149 in Slade et al. (2010).

150 **2.2.3. Heterotrophic bacteria counts and bacterial production**

151 For the enumeration of heterotrophic bacteria of discrete samples collected using the Niskin surface bottle

152 (<5m), subsamples (4.5mL) were fixed with glutaraldehyde grade I 25% (1% final concentration), and incubated

153 for 30 min at 4 °C, then quick-frozen in liquid nitrogen and stored at -80 °C until analysis. Samples were thawed

154 at room temperature. Counts were performed on a FACSCanto II flow cytometer (Becton Dickinson) equipped

155 with 3 air-cooled lasers: red (633 nm), blue (488 nm), red (633 nm) and violet (407 nm). For the enumeration of

156 heterotrophic bacteria, cells were stained with SYBR Green I (Invitrogen – Molecular Probes) at 0.025% (vol /

157 vol) final concentration for 15 min at room temperature in the dark. Stained cells were discriminated and

158 enumerated according to their right-angle light scatter (SSC) and green fluorescence using a 530/30 nm bandpass

159 filter. In a plot of green versus red fluorescence, heterotrophic bacteria were distinguished from autotrophic

160 prokaryotes. Fluorescent beads (1.002 µm; Polysciences Europe) were systematically added to each analyzed

161 sample as an internal standard. The cell abundance was determined from the flow rate, which was calculated

162 with TruCount beads (BD biosciences).

163 Heterotrophic prokaryotic production (BP) was estimated from rates of 3H leucine incorporation using the micro

164 centrifugation technique. The detailed protocol is available in Van wambeke et al (this issue). Briefly, triplicate

165 1.5 mL subsamples from the Niskin surface bottle (<5m) and one blank were incubated in the dark at in situ

166 temperature. Leucine was added at 20 nM final concentration and the leucine - carbon conversion factor used

167 was 1.5 kgC mol^{-1}

168 **2.3. Surface MicroLayer (SML) Sampling and Analysis**

169 **2.3.1. Sampling**

170 Surface microlayer SML sampling was conducted from a zodiac using a 50 x 26 cm silicate glass plate sampler

171 (Harvey 1966; Cunliffe and Wurl 2014) with an effective sampling surface area of 2600 cm^2 considering both

172 sides. For sampling, the zodiac was positioned 0.5 nautical miles away from the research vessel and into the

173 wind direction to avoid contamination. The glass plate was immersed perpendicular to the sea surface and
174 withdrawn at ~17 cm s^{-1}. SML samples were removed from the plate using a Teflon wiper (Cunliffe and Wurl,
175 2014) and collected in an acid cleaned and rinsed bottle. Prior to sampling, all equipment was cleaned with acid
176 (10 % HCl) and rinsed in MilliQ and copiously rinsed with seawater directly before samples were taken.
177

2.3.2. DOC analysis

179 The concentration of dissolved organic carbon (DOC) was determined in samples filtered online (Sartoban ©
180 300; 0.2 μm filters). Subsamples of 10 mL (in duplicate) were transferred to pre-combusted glass ampoules and
181 acidified with H_3PO_4 (final pH = 2). The sealed glass ampoules were stored in the dark at room temperature until
182 analysis. DOC measurements were performed on a Shimadzu TOC-V-CSH (Benner and Strom, 1993). Prior to
183 injection, DOC samples were sparged with CO_2 -free air for 6 min to remove inorganic carbon. A 100 μL aliquot
184 of samples were injected in triplicate and the analytical precision was 2%. Standards were prepared with
185 acetanilide. Analysis of DOC was performed both on SML and the underlying seawater sampled from the
186 zodiac.
187

2.4. Seaspray generation and analysis

2.4.1 General set-up

190 The sea spray generator has been characterized and deployed in a number of previous studies and full details are
191 reported in Schwier et al., (2015). Briefly, it consists of a 10 L glass tank, fitted with a plunging jet system for
192 the water. A particle-free air flushing system, placed perpendicular to the water surface at a distance of 1 cm to
193 send a constant airflow across the surface of the water to replicate the effects of wind on the surface of seawater.
194 The sea spray generator was supplied with a continuous flow of seawater collected at a depth of 5 m by an
195 underway seawater circulating system operated with a large peristaltic pump (Verder® VF40 with EPDM hose).

196 The different aerosol instrumentation, including a Time of Flight aerosol chemical speciation monitor (ToF-
197 ACSM), a differential mobility particle sizer (DMPS) coupled with a condensation particle counter (CPC), and
198 an impactor collected submicron particulate matter for offline ion chromatography analysis, sampled from the
199 headspace above the seawater in the tank. Two silica gel dryers were set up in series at the output of the
200 chamber. The aerosol relative humidity was measured continuously and varied from 20% to 40%. The total
201 sampling line length was approximately 2 m with a sampling flow of 5 L/min giving a residence time of less
202 than 30 seconds (Fig. S1). Regular tests were performed to ensure that the system was airtight and free from
203 external aerosol influences.

2.4.2 Aerosol physical and chemical properties

Size distribution measurements

206 Particle size distribution and number concentration measurements were obtained using the DMPS-CPC.
207 Measurements were provided approximately every 10 minutes for 25 different size classes ranging from 10 nm
208 up to 500 nm. The size distribution was relatively constant throughout the measurement period giving a principal
209 size mode at 110 nm and a second mode at 300 nm. This size distribution is characteristic of the bubbler
210 seawater generation method (Schwier et al., 2015), and is similar to that from other nascent seawater aerosol

211 generators (Bates et al., 2012), and to that observed in the clean marine boundary layer (Yoon et al., 2007).
212 Although the size distribution remained constant the absolute number concentration varied by a factor of 3 over
213 the sampling period. Details of these changes in aerosol number concentration as well as the associated cloud
214 condensation nuclei activity are detailed in a companion paper (Sellegri et al. submitted).

Offline PM1 filter analysis

216 In parallel to the online aerosol physical and chemical measurements, the generated nascent sea spray aerosol
217 particles were also sampled onto PM1 quartz filters. Aerosol samples were extracted in MilliQ water by
218 sonication (30 min) for the analysis of the water-soluble components. Extracts were analyzed by ion
219 chromatography for the quantification of the main inorganic ions (Sandrini et al., 2016). An IonPac CS16 3 ×
220 250 mm Dionex separation column with gradient MSA elution and an IonPac AS11 2 × 250 mm Dionex
221 separation column with gradient KOH elution were deployed for cations and anions, respectively. The water-
222 soluble organic carbon (WSOC) content of the extracts was quantified using a TOC thermal combustion analyzer
223 (Shimadzu TOC-5000A). Measurements of the total carbon (TC) content were performed on a filter punch cut
224 before water extraction by a thermal combustion analyzer equipped with a furnace for solid samples (Analytik
225 Jena, Multi NC2100S; Rinaldi et al., 2007). The punch was acidified before analysis to remove inorganic carbon
226 from TC and obtain TOC. Note that for some samples TC was measured also before acidification, allowing the
227 calculation of inorganic carbon content. The amount of inorganic carbon varies between 12 and 71% of TC, and
228 thus the acidification process for sea spray is an important step to follow for TOC measurements. Organic carbon
229 was converted to organic mass using conversion factors of 1.4 for the conversion of WIOC to WIOM, and 1.8
230 for the conversion of WSOC and WSOM, respectively (Facchini et al., 2008).

231 Although filters were only collected on a daily, they provided valuable information on the refractory component
232 of the aerosol population. The volume concentrations measured on the filters were similar to those calculated
233 from the DMPS (Fig. S2).

ToF-ACSM

235 The ToF-ACSM is based on the same operating principles as the aerosol mass spectrometer (Drewnick et al.,
236 2009). The ToF-ACSM contains a critical orifice, an aerodynamic lens to focus submicron particles into a
237 narrow beam that flows into a differentially pumped vacuum chamber, a heater (600°C) to vaporize particles, an
238 electron emitting tungsten filament (70eV) to ionize the vapor, a compact time-of-flight, mass analyzer (ETOF,
239 TOFWERK AG, Thun, Switzerland) and a discrete dynode detector (Fröhlich et al., 2013). It does not have the
240 ability to size aerosol particles but has the advantage of being more compact and more robust for continuous
241 observations than the AMS (Fröhlich et al., 2013). The ToF-ACSM alternates between sampling ambient air and
242 sampling through a filter in order to subtract the signal due to air.

243 During this experiment the ToF-ACSM was operated in a 2-min filter and 8-min sample mode with a
244 measurement every 10 minutes. The aerodynamic lens transmits particles between 70 nm and 700 nm, making
245 the ACSM approximately a PM1 measurement. The non-refractory particle material (NR-PM) is defined
246 similarly as in DeCarlo et al. (2006) as aerosol particles that are vaporized using the 600◦C resistively heated
247 vaporizer and detected during the instrument sampling interval. The relative ionization efficiency for NH_4 was
248 3.12 and for SO_4 0.8, determined from calibrations from ammonium sulfate and ammonium nitrate. The

249 temperature of the vaporizer and the size range do not permit efficient detection of sea salt particles. However, in
250 situations of high sea salt concentrations, detection of sea salt ions and related halides have been reported (Bates
251 et al., 2012; Giordano et al., 2017; Ovadnevaite et al., 2011; Schmale et al., 2013, Timonen et al., 2016).
252 Likewise, in this study mass spectral signals associated with sea salt were observed. In addition, the contribution
253 from chloride was very high (72% of the total mass). In some quadrupole ACSM instruments, negative Chl
254 peaks are often observed (Tobler et al., 2020), due to slow evaporation of refractory material from the vaporizer
255 relative to the 30 s switching time of filter and sample. This tends to overestimate the filter measurement and
256 underestimate the sample measurement and can lead to negative values for the difference. However, during these
257 measurements with the ToF-ACSM, negative Chl was not observed due to the long switching times.

258 The typical signature peaks for sea salt aerosol in our instrument were confirmed by atomizing pure aerosol
259 particles generated from sea salt solution (Biokar, synthetic sea salt, lot: 0017475), passing the particles through
260 a silica gel dryer and into the ToF-ACSM instrument. In the default fragmentation table used to assign the
261 signals at individual m/z's to chemical species (Allan et al., 2004), peaks associated with sea salt were identified
262 as organic aerosol fragments. In order to better represent the measured aerosol composition, we modified the
263 standard fragmentation table by introducing a sea salt species that includes m/z fragments at m/z 23 (Na^+), m/z
264 35 and 37 ($^{35}Cl^-$, $^{37}Cl^-$), 58 and 60 ($Na^{35}Cl$, $Na^{37}Cl$), and 81 and 83 ($NaCl_2$, $NaCl^{37}Cl$). For m/z 81, there is
265 overlap with an SO_4 fragment and a correction suggested by Schmale et al. (2013) was applied (Eq.1). This
266 correction accounted for less than 10% of the signal at m/z 81 and 3% of the total sulfate signal.

267 frag_SO4[81] = 81−frag_organic[81] −0.036×frag_Na[23]   (Eq.1)

268 Quantification of sea salt is difficult in the ToF-ACSM due to inefficient vaporization and a nonlinear
269 contribution to the Na^+ signal from surface ionization on the vaporizer. Therefore, in this work we do not attempt
270 to quantify the sea salt fraction, but instead use the mass spectral information to separate it from the organic
271 aerosols. A standard collection efficiency (CE) of 0.45 was applied to all data obtained from the ACSM
272 (Middlebrook et al., 2012). Regular periods of sampling with a filter in front of the ToF-ACSM were introduced
273 in order to ensure that there was no buildup of material on the vaporizer and that the sampling set up was leak-
274 free.

275 **Positive matrix factorization (PMF)**
276 In order to identify the different organic aerosols present in the sea spray from primary seawater, unconstrained
277 positive matrix factorization, using the SoFi interface (Canonaco et al., 2013) was performed on the ToF-ACSM
278 organic mass spectra. As described above, all sea salt related ions were removed from the organic mass spectral
279 data matrix, giving a total of 116 m/z from 0 up to 150. In addition, we removed the organic signal at m/z 29
280 because it is noisy due to a high background. The PMF solutions were explored up to eight factors. The four-
281 factor solution was chosen, based on correlations with reference mass spectra, and correlations with external
282 time series. The correlations for three to five factor solutions are illustrated in the supplementary material (Fig.
283 S3 to S5). The four identified factors, as well as their mass spectral fingerprints and time series will be discussed
284 in the following sections.

3. Results and discussions.

3.1. Time evolution of the chemical composition of nascent sea spray

Aerosol chemical composition obtained from the submicron offline filter measurements showed an average mass contribution is listed in Table 1. The soluble inorganic species concentrations were mostly found with proportions similar to the reference average seawater composition (Seinfeld and Pandis, 2006). However, enrichment in K^+ (69% of which was not explained by the average seawater composition) and a slight enrichment of Ca^{2+} was measured toward the end of the campaign (17% of Ca^{2+} was not explained by reference seawater composition from the 28th of May onward). In contrast, the magnesium was slightly depleted (20% less than expected in reference seawater composition) but less towards the end of the campaign. Filter-based organic matter (OM) was evenly composed of WIOM (14±5% of total mass) and WSOM (9%±5% of total mass), which contrasts with previous studies where organic matter in ambient marine aerosol was almost exclusively composed of WIOM (Facchini et al., 2008). However, these previous studies were conducted during phytoplankton bloom events of the Northern Atlantic Ocean, where POC is usually enhanced. Given that the Mediterranean Sea is characterized by oligotrophic conditions during PEACETIME, it could explain the relatively low contributions of WIOM.

Table 1. Concentrations of different chemical species in PM1 primary seawater aerosols measured using offline analysis of filters and online measurements from the ACSM.

offline analysis of filters ($\mu g\ m^{-3}$)		%	Non-refractory PM1 (ACSM) ($\mu g\ m^{-3}$)		%
SO_4^{2-}	1.53 ±0.7	7%	SO_4	0.18 ±0.15	3.2%
Na^+	4.86 ±1.9	21%	NO_3	0.02 ±0.02	0.1%
Cl-	10.4 ± 4.2	45%	NH_4	0.04 ±0.11	1.2 %
Ca^{2+}-	0.19 ± .07	0.07%	Seasalt	5.86 ±5	84%
K^+	0.11 ± 0.05	0.5%	Org	0.54±0.38	9.3%
Mg^+	0.50 ± 0.22	2%			
WIOM	3.13 ± 1.12	14M			
WSOM	2.02 ± 1.26	9M			

The chemical composition of SSA measured by the ACSM is shown in Fig. 2 and listed in Table 1 and was primarily composed of Sea Salt aerosol (determined from the signals at mz 23 (Na^+), 35 (Cl$^-$), 37(Cl-) 58(NaCl$^+$), 60(NaCl$^+$), 81(NaCl)Na$^+$ (84% ±15 %) followed by SO_4 concentrations at 3 %, and 9% organic matter.

307
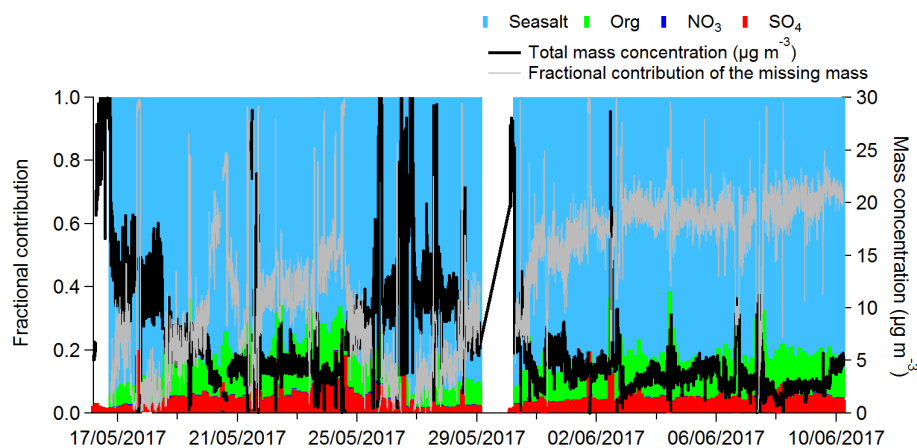
Figure 2: Time series of the fractional contribution of different species to the ToF-ACSM signal, as well as the total
mass concentrations measured by the ACSM (black), and the missing fraction (RefrMass) in grey.

308
309

310   In order to determine how representative the ACSM PM1 measurements were of the total PM1 mass, the total

311   ACSM PM1 mass concentration was converted into volume concentration (dividing organic mass concentrations

312   by a density value of 1.2 g cm^{-3} , and inorganic and sea salt components by 1.75 g cm^{-3} (Seinfeld and Pandis,

313   2006). This value was compared to the volume concentration measured by the DMPS-CPC, giving a correlation

314   (R) of 0.44, and slope (b) of 0.84 (Fig. 3). The agreement is relatively good in the first part of the transect, but

315   the difference between the ACSM-derived volume and the DMPS-derived volume increases over time. The

316   refractory material (Refr.) not measured by the ACSM is calculated as the difference between DMPS volume

317   concentration and ACSM volume concentration.
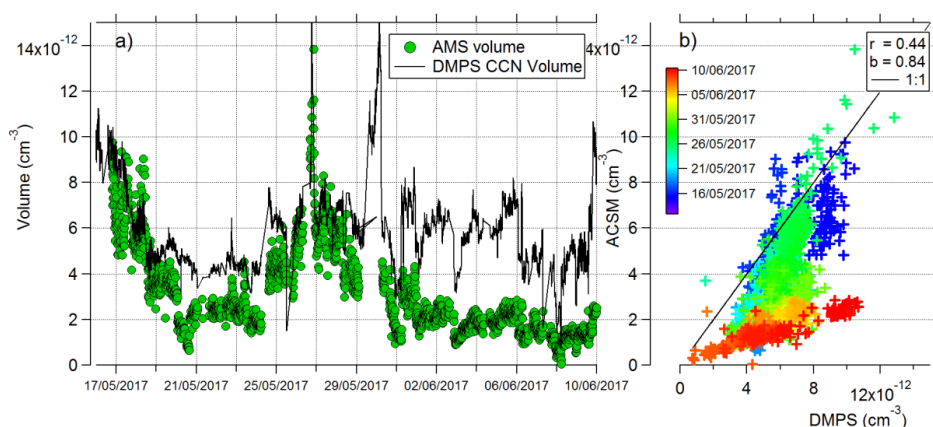
318
319   **Figure 3 Comparison between the ACSM and the DMPS volume concentration (#/cm cm^{-3}).**

320   The difference between the volume concentrations measured by the ACSM and SMPS were 44%±22%. NaCl

321   concentrations measured with the ACSM were in good agreement with the NaCl concentrations measured from

322   filters except during periods corresponding notably to the presence of the non-measured refractory mass (Fig

323   S6). This might suggest that the ability of the ACSM to measure NaCl particles depends on how NaCl is

324   associated with other compounds in the sea spray. Comparing this Refr. particle type to the different species

325   measured on the filters shows that it is reasonably correlated to the filter-based analysis of Mg^{2+}, Ca^{2+}, and NaCl.

326   Hence, it is possibly made of a mixture of carbonates from Ca^{2+}, Mg^{2+} and sea salt . (Fig S7). The PM1 mass

327   concentrations of OM calculated from the filters were additionally compared with the total OM measured from

328   the ACSM (OM_{ACSM}) (Fig. S8), the OM_{ACSM} was on average 80% lower than the total filter OM, indicating that

329   part of the refractory mass also contains organic matter. The temporal variation of the WSOM agreed better with

330   that of OM_{ACSM} than that of WIOM.

331   OM_{ACSM} varied from 0.2 to 1 µg m^{-3}, with higher concentrations measured in the North Western part of the ship

332   track. In the following section, we analyze in more detail the different organic aerosol species present in the

333   SSA samples and determine to what extent they are related to seawater biogeochemical properties.

3.2. Marine organic aerosol speciation

335   As explained in section 2 (Methodology), PMF was used to separate four organic factors. Based on correlations

336   with reference mass spectra we identified these factors as: an oxidized organic aerosol (OOA_{NR}), a somewhat

337   oxidized OA containing mixed amino acid and fatty acid signatures (MOA_{NR}); primary organics containing

338   aliphatic signature peaks as well as several peaks corresponding to fatty acids signatures (POA_{NR}), and a

339   methanesulphonic acid-like type OA ($MSA\text{-}OA_{NR}$) (Fig. 4). The correlations of each of the identified factors

340   with reference mass spectra are illustrated in Fig. S4. The OOA_{NR} contributed 51% ± 2% to OA and had

341   signature peaks with high m/z 44 and m/z 28. It did not contain any other m/z values that might suggest a

342   contribution from other species. The O/C ratio of the OOA_{NR} fraction was 1.6 (calculated using the method

343   described in Canagaratna et al., 2015), which is significantly higher than the average O/C ratio of LV-OOA

344   found in terrestrial ambient aerosols (0.8) (Canagaratna et al., 2015). High O/C ratios have been reported in

345   ambient studies where the carbonate species were thought to be measured by the ACSM (Bozzetti et al., 2017,

346   Vlachou et al., 2019). Thus the high O/C ratio observed for the OOA_{NR} organic class is not necessarily the

347   signature of the oxidation or processing of the primary organic matter.

348
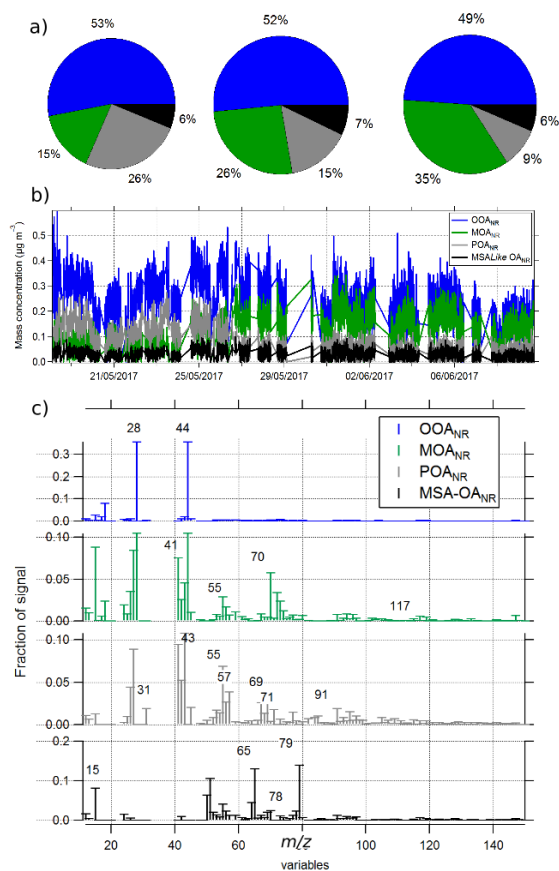
Figure 4 a) The contribution of the different organic factors the PEACETIME ship campaign, b) The mass concentrations of each factor (OOA$_{NR}$, MOA$_{NR}$, POA$_{NR}$ and MSA OA$_{NR}$) as a function of time, c) the mass spectra of the factors.

The second most dominant species was defined as a marine organic aerosol (MOA$_{NR}$). This factor contributed 15% to the total OA$_{NR}$ at the start of the campaign and then increased to 28% and 35% later on in the campaign (Fig. 4a). This MOA$_{NR}$ factor contained several mass peaks associated with amino acids (AA) reported in reference mass spectral signatures of leucine and valine respectively (Schneider et al., 2011)). AA signature peaks were identified at m/z 41 ($C_2H_3N^+$), 70, 98, 112 ($C_6H_{12}N_2^+$), 115, ($C_5H_9NO_2$), 117 ($C_5H_{11}NO_2$), 119 ($C_4H_9NO_3$), 131 ($C_6H_{13}NO_2$) and were similar to signature peaks that had been identified in previous studies by Schmale et al. (2013) in ambient marine aerosols and by Schneider et al. (2011) during a series of laboratory studies on different AA. Similar marker m/z's were present for fatty acid species such as those palmitic and oleic acid (Alfarra, PhD thesis 2004)). The MOA$_{NR}$ factor had an O/C of 0.53 and an H/C of 1.39, hence much less oxidized than the OOA$_{NR}$ type. These values are intermediate between those often calculated for low volatility, and semi-volatility OOA$_{NR}$ in the ambient atmosphere (Canagathna et al., 2015), and are similar to those identified by Schmale et al., 2013 for an amino acid type aerosol (O/C 0.35 and H/C 1.65) detected in an ambient aerosol.

365 The third most prominent factor was identified as a primary organic aerosol (POA$_{NR}$) and contributed 26% to the

366 total organics at the start of the campaign and decreased to 9% near the end of the campaign (Fig. 4b). This

367 factor contained typical aliphatic signatures and had little contribution from m/z 44. The mass spectral signature

368 of POA$_{NR}$ factor correlated well with reference mass spectra of leucine (R=0.56) and valine (r=0.51) but also

369 with fatty acid mass spectra, oleic (r=0.69), and palmitic acid (R= 0.74). The O/C ratio of this POA$_{NR}$ was 0.1

370 and the H/C was 1.64, which is typical for values of primary organic aerosol in the ambient atmosphere. The

371 POA$_{NR}$ factor identified in this work, as well as the H/C ratios, was similar to the aliphatic rich organic aerosol

372 species measured in contained wave chamber experiments during a phytoplankton bloom (Wang et al., 2015).

373 Once the bloom passed the H/C of these aerosol particles decreased, and it was hypothesized that the primary

374 organics were transformed through microbial activity in the water. During the PEACETIME campaign, the

375 POA$_{NR}$ factor had highest concentrations at the start of the field campaign and then later decreased to constant

376 values. This decrease in POA$_{NR}$ was accompanied by an increase in the more oxidized MOA$_{NR}$.

377 The last factor, MSA-OA$_{NR}$, contributed 6% ± 1% and contained typical signature peaks at m/z 65 (HSO$_2^+$), 79

378 (CH$_3$SO$_2^+$), and 96 (CH$_4$SO$_3^+$) similar to the mass spectral signatures identified by Timonen et al., (2016) in

379 Antarctica. However, unlike previously measured ambient MSA-*like* species (Schmale et al., 2013 Mallet et al.,

380 2019) it contained little or no oxygenated peaks at lower masses (m/z 43, 44, 45) making it impossible to

381 calculate an O/C ratio. However the H/C ratio of 1.12 was similar to 1.2 measured by Ovadnevaite et al. (2011),

382 but lower than the reported 1.6 by Schmale et al. (2011) for MSA-OA$_{NR}$, both detected in ambient aerosol. The

383 presence of an MSA-OA in nascent sea spray generated in the present study suggests that this compound is

384 already present in the seawater, and not only produced from gas-phase DMS emissions and oxidation in the

385 atmosphere. The Mediterranean Sea experiences a high level of radiation (Mermex 2011), and could also explain

386 the presence of MSA-like compounds from DMS oxidation within the seawater.

387 AA containing OA have been measured at a number of coastal sites, and their formation in the ambient

388 atmosphere is similar to that of MSA, where the AA are formed from the gas-phase partitioning of amines such

389 as trimethylamine or dimethylamine into the particulate phase (Facchini et al., 2008). However, a small number

390 of studies have identified these aerosol particle types directly from bubble bursting during controlled chamber

391 experiments (Dall'Osto et al., 2019; Kuznetsova et al., 2005; Decesari et al. 2019). These AA OA signatures

392 were detected during measurements made on the east coast of America, or in the Arctic (Dall'Osto et al, (2019),

393 and also during controlled wave chamber experiments (Wang et al, 2015).

394 In our experimental setup, the short time between particle generation and analysis (less than 30 seconds) does

395 not allow for the formation of secondary aerosol through the partitioning of gas-phase species into the particle

396 phase. Since these amino acid signatures are internally mixed with signatures for several different species, we

397 assume that they are present in the organic matter of the seawater, similar to conclusions made by Dall'Osto et

398 al. (2019).

399 OOA$_{NR}$ and MOA$_{NR}$ factors had a slight diurnal variation with increases during the early hours of the morning

400 and again in the afternoon (Fig 5). However given the low magnitude of the diurnal variation it is unlikely that

401 photochemical processes had a significant influence on the production of these species, and they are more likely

402 the result of processing of organic matter by microorganisms.

403

404
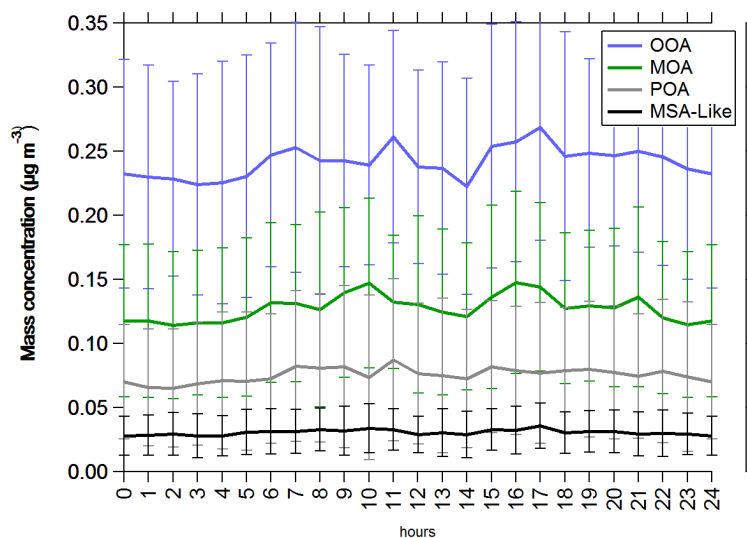
Figure 5: Diurnal variation of the four PMF organic factors chosen to represent the measured non refractory organic aerosol: average and standard deviation of the measurements during the whole PEACETIME cruise

3.3. The sources and formation pathways of marine organic aerosol species

407   In several large-scale climate models *Chl-a* is used as a proxy of phytoplankton biomass to predict the organic

408

409   fraction of sea spray. In this study, the measured *Chl-a* in the underway surface seawater was low and had little

410   variability (0.07 ± 0.013 mg m^{-3}), therefore making it difficult to extract any significant relationship between our

411   measured organic mass fractions and the measured *Chl-a*. No significant correlations were observed between the

412   mass concentrations of the OM, (measured by either the ACSM (OM$_{ACSM}$) or on filters (OM$_{filter}$

413   (WIOM+WSOM)) and *Chl-a* concentrations, nor between the fraction of these two organic classes to the total

414   seaspray mass and *Chl-a* (not shown). The fact that satellite-based, concurrently measured *Chl-a* may not be the

415   best surrogate for marine organic aerosol has been highlighted in previous studies (Rinaldi et al., 2013). This is

416   especially the case when little phytoplankton biomass is present. Therefore it is important to identify other

417   marker species or processes that can be used to correctly link seawater chemical composition, biological activity,

418   and the organic fraction in the seawater aerosol that can represent up to 20% of the total submicron sea spray

419   mass in oligotrophic waters.

420   In a companion paper, we illustrate that the total number of sea spray particles measured by the DMPS was

421   correlated to the nanophytoplankton cell abundance (NanoPhyto) (r=0.33, n 501, p <0.001), (Sellegri et al.

422   submitted). The hypothesis behind the dependence of the sea spray number concentration on NanoPhyto is that

423   organic matter released by NanoPhyto influences the surface seawater (SSW) surface tension, and therefore the

424   bubble lifetime that drives the number of film drops ejected to the atmosphere.

3.3.1. High time resolution correlations

In this section we will investigate the dependence of each of the organic classes identified in sea spray to the SSW biogeochemical properties. The relationships of the total organic mass concentrations and the fractional organic contributions to the seawater biochemistry were investigated (Fig; 6).
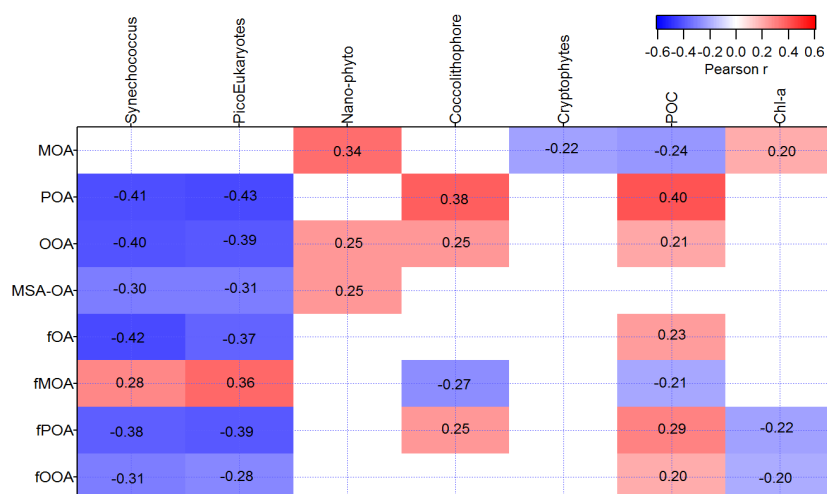
Figure 6: Pearson correlation matrix showing the agreement of the four different organic factors (MOA$_{NR}$, POA$_{NR}$, OOA$_{NR}$ and MSA-OA$_{NR}$) and their fraction to the total sea spray mass (fMOA, fPOA, fOOA and fOA) with several phytoplankton functional group abundance (cell. cm^3) (Synechococcus, PicoEukaryotes, NanoEukaryotes (Nano-Phyto), Coccolithophore (Coccolith), Cryptophytes), total Chl-a (mg.m^{-3}) and POC (μM) in the sampled seawater during the whole campaign. Sample number = 461, Correlations with R values < 0.16 had significance values lower than 0.001 and were therefore left blank.

MOA$_{NR}$ was strongly linked to NanoPhyto (r=0.34), as was MSA-OA$_{NR}$ and OOA$_{NR}$ but with less significance (r=0.25). Therefore, these organic classes follow the total sea spray mass and number behavior, as illustrated in Sellegri et al., (submitted). The hypothesis of organic matter influencing the surface tension of seawater, bubble lifetime, and the number of film drops, is therefore linked to this specific class of organic matter. Fatty acids, present in the MOA$_{NR}$ and OOA$_{NR}$ spectra, have been reported to be enriched in the SML (Cunliffe et al., 2012)), which would explain their impact on the bubble bursting process. POA$_{NR}$ species are instead significantly correlated with particulate organic carbon concentrations [POC] (r=0.40), and Coccolithophore like abundance (r=0.38) (Eq.2). A relationship between Coccolithophore-like cell abundance and [POC] is likely linked to the ability of the coccolithophores or similar groups of phytoplankton to secrete large amounts of sticky carbon which can result in the formation of gels and POC (Engel et al., 2004). As the time variation of POA$_{NR}$ does not follow that of total sea spray mass, it is possible that POA is not linked to film drops formation and is ejected into the atmosphere via separate mechanisms (such as jet drops). The time series of OOA$_{NR}$ had positive relationships with NanoPhyto (r=0.25), but also with coccolithophore-like cell abundances (r=0.25) and [POC] (r=0.21) and hence OOA$_{NR}$ seem to have an intermediate behavior between POA$_{NR}$ and MOA$_{NR}$. All organic classes except MOA$_{NR}$ are anticorrelated to the small classes of phytoplankton (picoeukaryotes and

synechococcus). This anticorrelation could be the result of the competition for nutrients between these small cells and the larger ones that rather drive the POC content.

Except for MOA$_{NR}$, all correlations for the absolute mass of these different types of organic matter are also observed when the fractional contribution of these species to the total mass of SSA (determined from the DMPS) are considered, although less significant (lower part of Fig.6). However, for MOA$_{NR}$ species, correlations with Nano-Phyto no longer hold if the fractional contribution of these species to the total mass of sea spray is considered. Instead, fMOA is correlated to picoeukaryotes and synechococcus. This is likely due to the strong anticorrelation of the fraction of all other organic classes with these small classes of phytoplankton. At low picoeukaryotes and Synechococcus cell abundances, fPOA, fOOA, and fMSA-OA are higher, artificially decreasing the proportion of fMOA to the rest of the organic matter.

3.3.2. Filter-based resolution correlations

Since the non-refractory organic components analyzed using the ACSM technique are only a fraction of the marine organic mass, we investigate the relationships between off-line filter-based organic compounds and seawater biogeochemical properties.
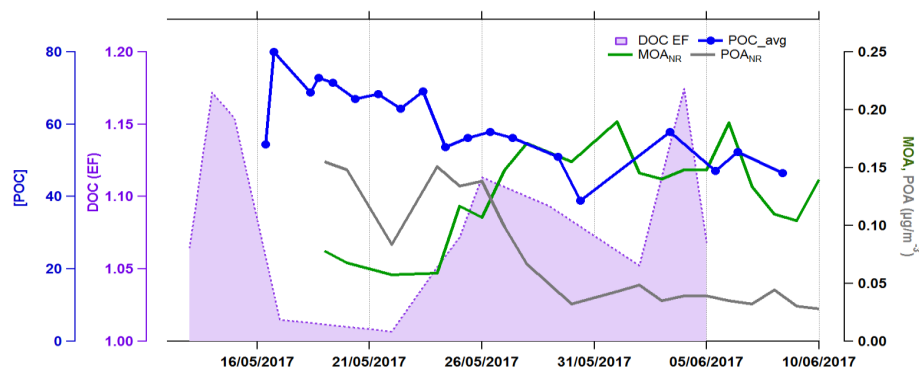
Figure 7. Time series of the DOC enrichment factor (EF), [POC] concentrations, and PMF organic factors MOA and POA.

Filter-based organic fractions are also compared to seawater properties at the filter sampling time resolution. The organic mass concentration from filters is correlated to the coccolithophore cell abundance (R=0.88, n=13). The fraction of OM to total mass analyzed on filters (OMSS) was also correlated to coccolithophore cell abundance (R=0.72, n=13) and POC (R=0.6, n=13). This indicates that the total organic matter present in sea spray behaved similarly to the non-refractory POA and OOA analyzed by the ACSM. Previous studies observed a connection between seawater POC and SSA organic fraction. Facchini et al. (2008) found that WIOM in SSA was related to seawater POC derived from microgels. Furthermore, during mesocosm bubbling experiments using *Emiliania huxleyi* cultures and low heterotrophic prokaryote abundance counts, O'Dowd et al., (2015) suggested that the aggregation of DOM into POC in the form of insoluble gel-colloids was the driving force behind the enrichment of organic matter into submicron SSA. The authors hypothesized that the organic fraction of SSA can be controlled either by DOC or POC, depending on the biological state of the waters.

480 Measurements of DOC in the SML and underlying seawater were performed daily, as well as surface seawater
481 bacterial total counts from daily CTD samples (surface water at 5m depth). DOC was slightly enriched in the
482 SML compared to the underlying seawater, with enrichment factors varying between 1 and 1.2 (Fig. 7). The
483 filter-based total organic content of sea spray aerosol was not correlated to DOC or total bacterial count in the
484 SML, neither was OMSS. However we observe that MOA_{NR} was correlated to the enrichment of DOC in the
485 SML (R=0.55, n= 9, p = 0.1), suggesting again that MOA_{NR} is likely linked to organic matter present in the
486 SML. The correlation between MOA and DOC enrichment in the SML suggests that the fraction of DOC which
487 is enriched in the SML contains lipids and amino acids found in the MOA_{NR} fraction. Although MOA_{NR} is an
488 oxidized organic class, it does not seem to be the result of the bacterial production (BP) of organic matter in the
489 seawater. We actually found a significant anticorrelation between MOA_{NR} and the bacterial production (R=-0.82,
490 n=10), indicating that MOA could instead be consumed by this process, while OMSS, positively correlated to
491 BP (R=0.68, n=10), would be a product of BP.

3.3.3. Predicting organic matter in sea spray from seawater biogeochemical properties

493 By combining relationships between filter-based chemical analysis, ACSM organic source apportionment and
494 seawater properties, it is possible to propose a general relationship that can be used to predict the different
495 fractions of organic matter in the nascent sea spray emitted from oligotrophic seawaters. These different organic
496 fractions may have different atmospheric properties related to their climate impact, such as ice nuclei properties
497 (Trueblood et al. in prep). We chose to parameterize the organic fractions of sea-spray rather than computing
498 organic mass fluxes, for an easier implementation in models that already have an inorganic sea spray source
499 function. However, as shown in the preceding section, the total mass of sea spray is significantly influenced by
500 SSW biology, and we recommend that the biology dependent sea spray number fluxes modulation computed in
501 Sellegri et al. (submitted) is applied before biology-dependent organic fractions are calculated.

502 The non-refractory organic fraction of nascent sea spray can be predicted with three different equations, with
503 $MSA\text{-}OA_{NR}$ being a negligible fraction of the total sea spray mass:

504 $\text{fPOA} = 0.0002\,[\text{POC}] - 0.001$ R =0.29 , n=459,p<0.001   Eq. 4

505 $\text{fOOA} = 0.0002\,[\text{POC}] + 0.02$ R=0.20, n=478, p < 0.001   Eq. 5

506 $\text{fMOA} = 4.5\ 10^{-6} \times (\text{picoeukaryotes}) + 0.009$ R=0.36, n=459, p < 0.001   Eq. 6

507 By subtracting all NR organic concentrations (ACSM measured) from the total filter-based organic
508 concentration, we obtain the refractory fraction of the organic matter (RefractOrg). This fraction dominates the
509 organic matter in sea spray. The fraction of RefractOrg to the total mass analyzed on filters (fRefraOrg) is
510 correlated to coccolithophores (R=0.82, n=11 p=0.001) and POC concentrations (R= 0.81, n= 10, p= 0.001),
511 similarly to the POA_{NR} and OOA_{NR} fractions of the sea spray, but with a better correlation to POC. Since POC
512 values are more available than coccolithophore numbers in models or satellite data, fRefraOrg can be computed
513 as follows:

514 $\text{fRefraOrg} = 0.005 \times [\text{POC}] - 0.11$ Eq.7

515   These relationships apply to the ranges of POC and picoeukaryotes measured during the PEACETIME cruise,
516   hence they may be applicable to other oligotrophic waters. If larger ranges of seawater biogeochemical
517   properties are considered in the future though, fractions of organic classes should be parameterized as
518   logarithmic laws asymptotic to 1, in order to take into account the saturation of the organic fraction at 1 for the
519   largest POC values.

520   **4. Conclusions**
521   The primary objective of this experiment was to study the relationships between sea spray chemical properties
522   and those of seawater. This work presents a unique dataset, which describes the first deployment of a ToF-
523   ACSM to characterize, in a continuous way, the organic fraction present in sea spray aerosol generated from
524   Mediterranean surface seawater. The non-refractory part of the organic content of sea spray was characterized by
525   low organic content and low variability along a 4300 km transect. Yet, using a positive matrix factorization on
526   the ACSM organic mass spectra, it was possible to extract signatures for fatty acids, amino acids, and marine
527   primary organic aerosols in non-refractory nascent sea spray. We identified four organic families: two were
528   composed of mixtures of amino acids and fatty acids (a primary aerosol POA_{NR}, and a slightly oxidized MOA_{NR}
529   factor), and two were identified as more oxidized organic aerosol (OOA_{NR} and MSA OA_{NR}). The POA_{NR} factor
530   was similar to that observed in wave chamber experiments and correlated well with POC concentrations in the
531   seawater, as did the OOA_{NR} and $MSA\text{-}OA_{NR}$. The MOA_{NR} concentrations had a different behavior and
532   correlated well with the nano-phytoplankton cell abundance in the seawater, and also with the total sea spray
533   number concentration and DOC enrichment in the surface microlayer. It is hypothesized that MOA_{NR} has surface
534   tension properties that influence the bubble bursting process and the resulting number of film drops ejected to the
535   atmosphere. In contrast, the fraction of POA, OOA and MSA classes are not connected to the sea spray number
536   concentration, but are linked to POC of the bulk surface seawater and more likely emitted with a different
537   process such as through jet drops.

538   Off-line chemical analysis of the submicron nascent sea spray provided a general view of the total organic
539   content of these particles, showing that a large part of the organic matter was refractory (to vaporization at
540   600°C) and thus not detected by the ACSM. However, this refractory organic matter within the nascent sea spray
541   was transferred to the atmospheric aerosol phase similarly to the POA_{NR} concentration found from the ACSM
542   analysis, being significantly correlated to the POC content of the bulk seawater.

543   This work illustrates the value of continuous aerosol chemistry and physical characterization of the nascent sea
544   spray aerosol in parallel with other biogeochemical measurements in surface seawater. It also illustrates that
545   even under oligotrophic conditions, seawater biogeochemical properties influence the type and concentration of
546   marine organic aerosols and therefore their ability to act as cloud condensation nuclei or ice nuclei. We provide a
547   parameterization of the different marine organic components of nascent sea spray as a function of seawater
548   biogeochemical properties typical for oligotrophic conditions in LNLC regions of the ocean that represents 60%
549   of the global ocean. Such parameterization used in models should allow a better prediction of the impact of
550   living marine organisms on these properties in a future climate.

Data availability: Underlying research data are being used by researcher participants of the "Peacetime" campaign to prepare other manuscripts, and therefore data are not publicly accessible at the time of publication. Data will be accessible (http://www.obs-vlfr.fr/proof/php/PEACETIME/peacetime.php, last access: 22 June 2020) once the special issue is completed (all papers should be published by fall 2020). The policy of the database is detailed here http://www. obs-vlfr.fr/proof/dataconvention.php (last access: 22 June 2020).

Acknowledgments
This study is a contribution to the PEACETIME project (http://peacetime-project.org), a joint initiative of the MERMEX and ChArMEx components supported by CNRS-INSU, IFREMER, CEA, and Météo-France as part of the programme MISTRALS coordinated by INSU. PEACETIME was endorsed as a process study by GEOTRACES. PEACETIME cruise https://doi.org/10.17600/17000300. Sea2Cloud was endorsed by SOLAS;We thank the captain and the crew of the RV Pourquoi Pas ? for their professionalism and their work at sea.

Author contributions: CG and KD designed the PEACETIME project. KS designed the experiments specifically used in this manuscript. KS and AN performed the measurements aboard the ship. MT, GG, NH, JD, IO, F V-W, A.E and BZ were responsible for collecting and analyzing the biogeochemical parameters in either the seawater or in the surface microlayer. MR analyzed the offline filter measurements. EF analyzed the ACSM data with input from LW and ASHP. EF and KS prepared the manuscript with contributions from all authors.

References:

Allan, J.D., Delia, A.E., Coe, H., Bower, K.N., Alfarra, M.R., Jimenez, J.L., Middlebrook, A.M., Drewnick, F., Onasch, T.B., Canagaratna, M.R. A generalised method for the extraction of chemically resolved mass spectra from Aerodyne aerosol mass spectrometer data. J. Aerosol Sci. 35, 909–922. https://doi.org/10.1016/j.jaerosci.2004.02.007, 2004

Bates, T., Quinn, P., Frossard, A., Russell, L., Hakala, J., Petäjä, T., Kulmala, M., Covert, D., Cappa, C., Li, S. Measurements of ocean derived aerosol off the coast of California. J. Geophys. Res Atmos 117. https://doi.org/10.1029/2012JD017588, 2012

Benner R, Strom M. A critical evaluation of the analytical blank associated with DOC measurements by high temperature catalytic oxidation. Mar Chem 41:153–160, https://doi.org/10.1016/0304-4203(93)90113-3, 1993

Boss,E, M. Picheral, T. Leeuw, A. Chase, E. Karsenti, G. Gorsky, L. Taylor, W. Slade, J. Ras, H. Claustre. The characteristics of particulate absorption, scattering and attenuation coefficients in the surface ocean; Contribution of the Tara Oceans expedition, *Methods in Oceanography*. 7, 52-62, https://doi.org/10.1016/j.mio.2013.11.002, 2013

Burrows, S. M., Ogunro, O., Frossard, A. A., Russell, L. M., Rasch, P. J., and Elliott, S. M.: A physically based framework for modeling the organic fractionation of sea spray aerosol from bubble film Langmuir equilibria, Atmos. Chem. Phys., 14, 13601–13629, https://doi.org/10.5194/acp-14-13601-2014, 2014.

Blanchard, D.C., Woodcock, A.H. The production, concentration, and vertical distribution of the sea-salt aerosol. The. N. Y. Acad. Sci. 338, 330–347. https://doi.org/10.1111/j.1749-6632.1980.tb17130.x, 1980

588   Bozzetti, C., I. El Haddad, D. Salameh, K. R. Daellenbach, P. Fermo, R. Gonzalez, M. C. Minguillon, Y. Iinuma,
589   L. Poulain, M. Elser, E. Muller, J. G. Slowik, J. L. Jaffrezo, U. Baltensperger, N. Marchand, and A. S.
590   H. Prevot. Organic aerosol source apportionment by offline-AMS over a full year in Marseille, Atmos.
591   Chem. Phys., 17, 8247–8268, https://doi.org/10.5194/acp-17-8247-2017, 2017

592   Canagaratna, M., Jimenez, J., Kroll, J., Chen, Q., Kessler, S., Massoli, P., Hildebrandt Ruiz, L., Fortner, E.,
593   Williams, L., Wilson, K., 2015. Elemental ratio measurements of organic compounds using aerosol
594   mass spectrometry: characterization, improved calibration, and implications. Atmos. Chem. Phys., 15,
595   253–272, https://doi.org/10.5194/acp-15-253-2015, 2015.

596   Canonaco, F., Crippa, M., Slowik, J., Baltensperger, U., Prévôt, A.S., 2013. SoFi, an IGOR-based interface for
597   the efficient use of the generalized multilinear engine (ME-2) for the source apportionment: ME-2
598   application to aerosol mass spectrometer data. Atmos. Meas. Tech., 6, 3649–3661,
599   https://doi.org/10.5194/amt-6-3649-2013, 2013.

600   Cetinic, M. J. Perry, N. T. Briggs, E. Kallin, E. A. D'Asaro, and C. M. Lee , Particulate organic carbon and
601   inherent optical properties during 2008 North Atlantic bloom experiment, *J. Geophys Res-Oceans;*
602   *Geophysical Research: Oceans*, 117 (6), doi:10.1029/2011JC007771, 2012.

603   Christaki, U., Courties, C., Massana, R., Catala, P., Lebaron, P.,Gasol, P., and Zubkov, M. V. Optimized routine
604   flow cytometric enumeration of heterotrophic flagellates using SYBR Green I, Limnol. Oceanogr.
605   Meth, 9, 329–339. https://doi.org/10.4319/lom.2011.9.329, 2011.

606   Cunliffe, M., Engel, A., Frka, S, Gasparovic, B, Guitart, C., Murrell, C., Salter, M., Stolle, C. , Upstill-Goddard
607   R., and Wurl, O. Sea surface microlayers: A unified physiochemical and biological perspective of the
608   air-ocean interface. Prog Oceanogr, 109, 104-116, https://doi.org/10.1016/j.pocean.2012.08.004, 2013.

609   Cunliffe, M., and Wurl, O. Guide to best practices to study the ocean's surface. Plymouth, UK, Marine
610   Biological Association of the United Kingdom for SCOR, 118pp. (Occasional Publications of the
611   Marine Biological Association of the United Kingdom). http://hdl.handle.net/11329/261, 2014;

612   Dall'Osto, M., Airs, R.L., Beale, R., Cree, C., Fitzsimons, M.F., Beddows, D., Harrison, R.M., Ceburnis, D.,
613   O'Dowd, C., Rinaldi, M. Simultaneous detection of alkylamines in the surface ocean and atmosphere of
614   the Antarctic sympagic environment. ACS Earth Space Chem. 3, 854–862.
615   https://doi.org/10.1021/acsearthspacechem.9b00028, 2019

616   Decesari, S., Paglione, M. Rinaldi, M., Dall'Osto, M., Simó, R., Zanca, N., Volpi, F., Facchini, M-C., Hoffmann,
617   T., Götz, S., Kampf, K.J, O'Dowd, C., Ovadnevaite, J., Ceburnis, D., and Tagliavini, E. Shipborne
618   measurements of Antarctic submicron organic aerosols: an NMR perspective linking multiple sources
619   and bioregions Atmos. Chem. Phys. Discuss., https://doi.org/10.5194/acp-2019-888, 2019

620   Drewnick, F., Hings, S. S., Alfarra, M. R., Prevot, A. S. H., and Borrmann, S.: Aerosol quantification with the
621   Aerodyne Aerosol Mass Spectrometer: detection limits and ionizer background effects, Atmos. Meas.
622   Tech., 2, 33–46, https://doi.org/10.5194/amt-2-33-2009, 2009.

623   Engel, A., Delille, B., Jacquet, S., Riebesell, U., Rochelle-Newall, E., Terbrüggen, A., Zondervan, I. Transparent
624   exopolymer particles and dissolved organic carbon production by Emiliania huxleyi exposed to

different CO2 concentrations: a mesocosm experiment. Aquat. Microb. Ecol. 34, 93–104. DOI: 10.3354/ame034093, 2004

Facchini, M.C., Rinaldi, M., Decesari, S., Carbone, C., Finessi, E., Mircea, M., Fuzzi, S., Ceburnis, D., Flanagan, R., Nilsson, E.D. Primary submicron marine aerosol dominated by insoluble organic colloids and aggregates. Geophys. Res. Lett. 35. https://doi.org/10.1029/2008GL034210, 2008

Fröhlich, R., Cubison, M. J., Slowik, J. G., Bukowiecki, N., Prévôt, A. S. H., Baltensperger, U., Schneider, J., Kimmel, J. R., Gonin, M., Rohner, U., Worsnop, D. R., and Jayne, J. T.: The ToF-ACSM: a portable aerosol chemical speciation monitor with TOFMS detection, Atmos. Meas. Tech., 6, 3225–3241, https://doi.org/10.5194/amt-6-3225-2013, 2013.

Guieu, C., D'Ortenzio, F., Dulac, F., Taillandier, V., Doglioli, A., Petrenko, A., Barrillon, S., Mallet, M., Nabat, P., and Desboeufs, K.: Process studies at the air-sea interface after atmospheric deposition in the Mediterranean Sea: objectives and strategy of the PEACETIME oceanographic campaign (May–June 2017), Biogeosciences Discuss., https://doi.org/10.5194/bg-2020-44, in review, 2020.

Giordano, M. R., Kalnajs, L. E., Avery, A., Goetz, J. D., Davis, S. M., and DeCarlo, P. F.: A missing source of aerosols in Antarctica – beyond long-range transport, phytoplankton, and photochemistry, Atmos. Chem. Phys., 17, 1–20, https://doi.org/10.5194/acp-17-1-2017, 2017.

Harvey, G. Microlayer collection from the sea surface: a new method and intial results. *Limnol. Ocean* 11, 608–613. doi: 10.4319/lo.1966.11.4.0608, 1966

Kuznetsova, M., Lee, C., Aller, J. Characterization of the proteinaceous matter in marine aerosols. Mar. Chem. 96, 359–377. https://doi.org/10.1016/j.marchem.2005.03.007, 2005

Leroux, R., G. Grégori, K. Leblanc, F. Carlotti, M. Thyssen, M. Dugenne, M. Pujo-Pay, P. Conan, M.-P. Jouandet , N. Bhairy, L. Berline Combining laser diffraction, flow cytometry and optical microscopy to characterize a nanophytoplankton bloom in the northwestern Mediterranean. *Prog Oceanogr*, 163, 248-259. https://doi.org/10.1016/j.pocean.2017.10.010, 2017.

McCluskey, C.S., Hill, T.C., Malfatti, F., Sultana, C.M., Lee, C., Santander, M.V., Beall, C.M., Moore, K.A., Cornwell, G.C., Collins, D.B.. A dynamic link between ice nucleating particles released in nascent sea spray aerosol and oceanic biological activity during two mesocosm experiments. J. Atmospheric Sci. 74, 151–166. *https://doi.org/10.1175/JAS-D-16-0087.1*, 2017.

MerMex Group, Marine ecosystems' responses to climatic and anthropogenic forcings in the Mediterranean, Prog Oceanogr doi:10.1016/j.pocean.2011.02.003, 91 (2011) 97–166 https://doi.org/10.1016/j.pocean.2011.02.003, 2011.

Middlebrook, A.M., Bahreini, R., Jimenez, J.L., Canagaratna, M.R. Evaluation of composition-dependent collection efficiencies for the aerodyne aerosol mass spectrometer using field data. Aerosol Sci. Technol. 46, 258–271. https://doi.org/10.1080/02786826.2011.620041, 2012.

O'Dowd, C.D., Facchini, M.C., Cavalli, F., Ceburnis, D., Mircea, M., Decesari, S., Fuzzi, S., Yoon, Y.J., Putaud, J.-P. Biogenically driven organic contribution to marine aerosol. Nature 431, 676. DOI:10.1038/nature02959, 2004.

663 O'Dowd, C., Ceburnis, D., Ovadnevaite, J. *et al.* Connecting marine productivity to sea-spray *via* nanoscale
664 biological processes: Phytoplankton Dance or Death Disco?. *Sci Rep* 5, 14883.
665 https://doi.org/10.1038/srep14883, 2015.

666 Ovadnevaite, J., O'Dowd, C., Dall'Osto, M., Ceburnis, D., Worsnop, D.R., Berresheim, H. Detecting high
667 contributions of primary organic matter to marine aerosol: A case study. Geophys. Res. Lett. 38.
668 DOI: 10.1029/2010GL046083, 2011

669 Rinaldi, M. et al. Chemical characterization and source apportionment of size-segregated aerosol collected at an
670 urban site in Sicily. Water Air Soil Poll 185, 311–21, doi:10.1007/s11270-007-9455-4, 2007.

671 Rinaldi, M., Fuzzi, S., Decesari, S., Marullo, S., Santoleri, R., Provenzale, A., Von Hardenberg, J., Ceburnis, D.,
672 Vaishya, A., O'Dowd, C.D. Is chlorophyll-a the best surrogate for organic matter enrichment in
673 submicron primary marine aerosol? J. Geophys. Res. Atmos 118, 4964–4973.
674 https://doi.org/10.1002/jgrd.50417, 2013.

675 Sandrini, S. et al. Size-resolved aerosol composition at an urban and a rural site in the Po Valley in summertime:
676 implications for secondary aerosol formation. Atmos. Chem. Phys. 16, 10879–10897, doi:10.5194/acp-
677 16-10879-2016, 2016.

678 Schmale, J., Schneider, J., Nemitz, E., Tang, Y. S., Dragosits, U., Blackall, T. D., Trathan, P. N., Phillips, G. J.,
679 Sutton, M., and Braban, C. F.: Sub-Antarctic marine aerosol: dominant contributions from biogenic
680 sources, Atmos. Chem. Phys., 13, 8669–8694, https://doi.org/10.5194/acp-13-8669-2013, 2013.

681 Schneider, J., Freutel, F., Zorn, S. R., Chen, Q., Farmer, D. K., Jimenez, J. L., Martin, S. T., Artaxo, P.,
682 Wiedensohler, A., and Borrmann, S.: Mass-spectrometric identification of primary biological particle
683 markers and application to pristine submicron aerosol measurements in Amazonia, Atmos. Chem.
684 Phys., 11, 11415–11429, https://doi.org/10.5194/acp-11-11415-2011. 2011.

685 Schwier, A. N., Rose, C., Asmi, E., Ebling, A. M., Landing, W. M., Marro, S., Pedrotti, M.-L., Sallon, A.,
686 Iuculano, F., Agusti, S., Tsiola, A., Pitta, P., Louis, J., Guieu, C., Gazeau, F., and Sellegri, K.: Primary
687 marine aerosol emissions from the Mediterranean Sea during pre-bloom and oligotrophic conditions:
688 correlations to seawater chlorophyll *a* from a mesocosm study, Atmos. Chem. Phys., 15, 7961–7976,
689 https://doi.org/10.5194/acp-15-7961-2015, 2015.

690 Seinfeld and Pandis, Atmospheric Chemistry and Physics: From Air Pollution to Climate Change, Third edition,
691 Hoboken, New Jersey : John Wiley &, Sons, Inc., [2016] ©2016

692 Sellegri K., Nicosia, A., Freney, E., Uitz, J, Thyssen, M.,, Grégori, G., Engel, A., Zäncker, B., Haëntjens, N.,
693 Mas, S., Picard, D., Saint-Macary, A., Peltola, M., Rose, C , Trueblood, J.T, Lefevre, D.,D'Anna, B.,
694 Desboeuf, K., Meskhidze, N., Guieu, C and Law, C. S., Surface ocean microbiota determine cloud
695 precursors, submitted

696 Slade, W.H, Boss, E., Dall'Olmo,G., Langner, M.R., Loftin,J., Behrenfeld, M.J. and Roesler, C., Underway and
697 moored methods for improving accuracy in measurement of spectral particulate absorption and

698   attenuation. J Atmos Ocean Tech, 27:10, 1733-1746.
699   *https://doi.org/10.1175/2010JTECHO755.1, 2010*

700 Tobler, A. K, Skiba, A, Wang, D.S, Croteau, P, Styszko, K, Nęcki, J, Baltensperger, U, Slowik, J.G., and
701   Prévôt A.S. H.. Improved chloride quantification in quadrupole aerosol chemical speciation monitors
702   (Q-ACSMs), submitted to Atmos. Meas Tech.

703 Thyssen, M., G. Grégori, J -M Grisoni, M. Pedrotti, L. Mousseau, L.F. Artigas, S. Marro, N. Garcia, O.
704   Passafiume and M.J. Denis, Onset of the spring bloom in the northwestern Mediterranean Sea :
705   influence of environmental pulse events on the in situ hourly-scale dynamics of the phytoplankton
706   community structure. *Front. Microbiol.* 5:387. doi:10.3389/fmicb.2014.003872014, 2010.

707 Timonen, H., Cubison, M., Aurela, M., Brus, D., Lihavainen, H., Hillamo, R., Canagaratna, M., Nekat, B.,
708   Weller, R., Worsnop, D., and Saarikoski, S.: Applications and limitations of constrained high-resolution
709   peak fitting on low resolving power mass spectra from the ToF-ACSM, Atmos. Meas. Tech., 9, 3263–
710   3281, https://doi.org/10.5194/amt-9-3263-2016, 2016.

711 Trueblood, J. T, Nicosia̓ A., Engel, A, Zäncker, B., Rinaldi̓ M., Freney̓ E, Thyssen, M, Obernosterer̓ I,
712   Dinasquet, J, Haëntjens, N, Belosi, F, Santachiara, G, Guieu, C, and Sellegri, K.̓ A Two-Component
713   Parameterization of Marine Ice Nucleating Particles Based on Seawater Biology and Sea Spray Aerosol
714   Measurements During the PEACETIME Cruise in the Mediterranean Sea, in prep, 2020

715 Vlachou, A., Tobler, A., Lamkaddam, H., Canonaco, F., Daellenbach, K. R., Jaffrezo, J.-L., Minguillón, M. C.,
716   Maasikmets, M., Teinemaa, E., Baltensperger, U., El Haddad, I., and Prévôt, A. S. H.: Development of
717   a versatile source apportionment analysis based on positive matrix factorization: a case study of the
718   seasonal variation of organic aerosol sources in Estonia, Atmos. Chem. Phys., 19, 7279–7295,
719   https://doi.org/10.5194/acp-19-7279-2019, 2019.

720 Wang, X., Sultana, C.M., Trueblood, J., Hill, T.C., Malfatti, F., Lee, C., Laskina, O., Moore, K.A., Beall, C.M.,
721   McCluskey, C.S. Microbial control of sea spray aerosol composition: a tale of two blooms. ACS Cent.
722   Sci. 1, 124–131. https://doi.org/10.1021/acscentsci.5b00148, 2015.

723 Yoon, Y., Ceburnis, D., Cavalli, F., Jourdan, O., Putaud, J., Facchini, M., Decesari, S., Fuzzi, S., Sellegri, K.,
724   Jennings, S. Seasonal characteristics of the physicochemical properties of North Atlantic marine
725   atmospheric aerosols. J. Geophys. Res. Atmos 112.
726   https://doi.org/10.1029/2005JD007044, 2007

727

728